Analyst

ROYAL SOCIETY OF CHEMISTRY

PAPER

View Article Online
View Journal | View Issue

Cite this: *Analyst*, 2022, **147**, 3494

Construction of dPCR and qPCR integrated system based on commercially available low-cost hardware

Kangning Wang,†[a] Benliang Sang,†[b,d] Limin He,[b,d] Yu Guo,[c] Mingkun Geng,[b,d] Dezhou Zheng,[e] Xiaolong Xu[f] and Wenming Wu*[a]

Received 23rd April 2022,
Accepted 22nd June 2022

DOI: 10.1039/d2an00694d

rsc.li/analyst

Fluorescent quantitative PCR (qPCR) and digital PCR (dPCR) are two mainstream nucleic acid quantification technologies. However, commercial dPCR and qPCR instruments have a low integration, a high price, and a large footprint. To solve these shortcomings, we introduce a compound PCR system with both qPCR and dPCR functions. All the hardware used in this compound PCR system is commercially available and low-cost, and free software was used to realize the absolute quantification of nucleic acids. The compound PCR provides two working modes. In the qPCR mode, thermal cycling is realized by controlling the reciprocating motion of the *x* axis. The heating rate is 1.25 °C s^{-1} and the cooling rate is 1.75 °C s^{-1}. We performed amplification experiments of the PGEM-3zf (+)1 gene. The performance level was similar to commercial qPCR instruments. In the dPCR mode, the heating rate is 0.5 °C s^{-1} and the cooling rate is 0.6 °C s^{-1}. We performed the UPE-Q gene amplification and used the sequential actions of the two-dimensional mechanical sliders to scan the reaction products and used the method of regional statistics and back-inference threshold to get test results. The result we got was 1208 copies per μL^{-1}, which was similar to expectations.

Introduction

The PCR reaction is a molecular biology method to expand specific DNA fragments *in vitro*. In 1971, Khorana *et al.*[1] proposed the principle of *in vitro* expansion of nucleic acids, but it had not received much attention due to experimental conditions required and the limitations of the reagents. It was not until 1985 that R. K. Saiki *et al.*[2] published the first research article on PCR, which marked the official birth of the technology. The reaction principle of PCR is similar to DNA replication in living organisms. The major difference is that the environment of the PCR reaction is *in vitro*. A PCR amplification reaction mainly includes three stages. (1) A denaturation step where the template DNA is denatured at 95 °C and the double-stranded structure opens to form a single strand. (2) An annealing step where the temperature is lowered to about 55 °C so that primers can bind to a single strand of DNA according to the principle of base pairing. (3) An extension step around 72 °C where, under the action of a Taq enzyme, dNTPs are incorporated to synthesize the complementary strand of the template by extending it from the 3′ end in the 5′ → 3′ direction. After more than 30 years of development, PCR is widely used in agriculture,[3–5] food testing,[6–8] and in medical diagnosis,[9–11] for instance.

The development of PCR instruments has reached its third generation: end-point PCR, real-time PCR (qPCR), and digital PCR (dPCR). All three generations achieve gene amplification through a specific temperature cycle, but there are great differences in the quantification method of the DNA. The end-point PCR instrument does not quantify the DNA in the samples, whereas a real-time PCR instrument can achieve it using an integrated fluorescence detection module, for in-stance. Compared with the previous two generations of PCR instruments, digital PCR has the most advanced detection and quantification. It is the only way to absolutely quantify the nucleic acids and its detection sensitivity is far greater than for the traditional method.[12] However, a disadvantage of a digital PCR system is the relatively narrow range of nucleic acid concentrations that can be detected. Besides, the detection range is controlled by the number of droplets. Commercial dPCR

[a]*Institute of biological and medical engineering, Guangdong Academy of Sciences, China. E-mail: wuwenming627@163.com*
[b]*Changchun Institute of Optics, Fine Mechanics and Physics (CIOMP), Chinese Academy of Sciences, China*
[c]*School of Mechanical and Electrical Engineering, Guangdong University of Technology, China*
[d]*University of Chinese Academy of Sciences (UCAS), Beijing, China*
[e]*College of Applied Physics and Materials, Wuyi University, China*
[f]*School of Biotechnology and Health Sciences, Wuyi University, China*
†These authors contributed equally to this work.

instruments (Applied Biosystems, Inc. or Bio-Rad) have a nucleic acid detection range of only four orders of magnitude, but real-time fluorescent PCR can detect nucleic acids of up to ten orders of magnitude.

There are advantages and disadvantages to both PCR quantification techniques. A digital PCR instrument generally needs a customized microfluidic chip,[13–15] which adds to its already high cost. In contrast, real-time fluorescent PCR instruments generally do not need any customized microfluidic chip and when a chip is needed, it can usually be manufactured at a very low cost.[16,17] Therefore, compared to dPCR, a single test costs much less with a real-time fluorescent PCR. In terms of sensitivity, real-time fluorescent PCR instruments can easily distinguish twice the concentration difference, but the performance is lower at low concentrations. In theory, digital PCR can achieve trace detection of a single nucleic acid molecule since the detection is extremely sensitive.[12] The reaction flux of a real-time fluorescent PCR instrument makes it easier to achieve high throughput, unlike digital PCR. By comparing dPCR and real-time fluorescent PCR instruments, there is a strong complementarity between both instruments. Therefore, it appears very useful to a compound PCR instrument that combines both the characteristics.

Recently, a large number of studies have been published that highlight efficient approaches. Salman *et al.*[18] designed a shunting microfluidic PCR instrument that can rapidly detect bacteria. They used a rotational servo motor to move the reagents inside three temperature areas to achieve temperature cycling. Using mechanical movement to create a temperature cycle achieves high temperature rates and a flexible adjustment of the temperature holding times. Besides, the mechanical movement control is simple and easy to realize. However, such a system is unable to achieve rapid temperature rise and fall and it is limited to the applications of end point PCR and does not implement the evolutions brought by the second-and third-generation instruments. Zhou *et al.*[19] designed a real-time digital PCR system using TECs uses for temperature cycling and fluorescence detection for real-time monitoring. This system can distinguish between false positives and false negatives. However, the resolution of the optical system they designed is not high enough, and for chips with a number of microcavities up to 10 000, it is impossible to achieve good detection.

These previous studies have designed some novel PCR systems, but there are still many challenges remaining to integrate qPCR and dPCR. First, all three functional units of a digital PCR instrument are difficult to integrate. They consist of a droplet generation unit, a gene amplification unit, and a fluorescence detection unit that all have completely different structures. To our knowledge, there have been no reports of a successful development of a highly integrated and fullyautomated digital PCR platform. Second, qPCR and dPCR have different fluorescence detection methods, which makes it difficult to implement both detection methods on a single device. A compound PCR instrument needs real time fluorescence detection as well as a precise end point fluorescence detection. In particular, for the end point fluorescence detection, droplets at different positions on the chip receive uneven light, which can easily cause statistical errors that are hard to eliminate. In this work, we introduce a compound PCR system that integrates qPCR and dPCR functions using a two dimensional mechanical slide to achieve stable thermal cycling and scanning fluorescence detection. This PCR instrument solves the problems of the difficult integration of dPCR and low fluorescence detection limits by merging qPCR and dPCR.

Materials and methods

Reagents

To verify the qPCR and dPCR functions, we carried out corresponding tests. The reagents used in the qPCR include 10 μL of premix, 6 μL of water, 2 μL of forward and reverse primers, 1 μL of EvaGreen Dye, and 2 μL of PGEM-3ZF (+) 1 plasmid. The sequence of the PGEM-32ZF (+)1 forward primer is: CCAGTCGGGAAACCTGTCGTGCC and that of the reverse primer is: GTGAGCGAGGAAGCGGAAGAGCG. The reagents used in the dPCR include 10 μL of premix, 8 μL of water, 0.75 μL of forward and reverse primers, 0.5 μL of probes, and 2 μL of UPE-Q plasmids. The forward primer sequence of UPE-Q is: GCAACGCGCGATTCAGTT and that of the reverse primer is: GCCTCTACACGGGACCCATA. The probe sequence for UPE-Q is: CTCTTCACATAATCGCCCCGAGCTCG.

Microfluidic chips

Chips for the qPCR mode. The chips used in the qPCR and dPCR modes are different. In the qPCR mode, we used a home-made chip (Fig. 1a). PDMS(polydimethylsiloxane) is widely used in microfluidics.[20–22] We cut the cured PDMS into an appropriate size determined according to the reaction flux, punched four small holes on its surface determined according to the reaction flux, and bonded it with glass using plasma. The chip is simple to fabricate and comes at a low cost, additionally, high throughput experiments can be made by increasing the number of holes. During their addition, it is necessary to pay attention to the order of the reagent. Firstly, we injected 2.5 μL of mineral oil into the reaction chamber, then 1.5 μL of reagents into the mineral oil.

Table 1 shows that the total price of the parts of the self-made fluorescence detection equipment is 957 US dollars. The price of commercial real-time fluorescence detection equipment is about 35 000 US dollars, and even the price of digital PCR equipment is about 180 000 US dollars. Through comparison, it is found that the cost of self-developed PCR is far lower than that of commercial PCR equipment.

Chips for the dPCR mode. In the dPCR mode, the compound PCR instrument uses a Quantstudio 3D Digital PCR chip (Fig. 1b). The digital PCR chip has 20 000 microcavities with a total size of 10 × 10 mm. The operation of this chip is relatively simple and can be realized manually. The reagent addition process is as follows. First, a droplet of the reagent is added onto a dedicated loader, then the loader is used to

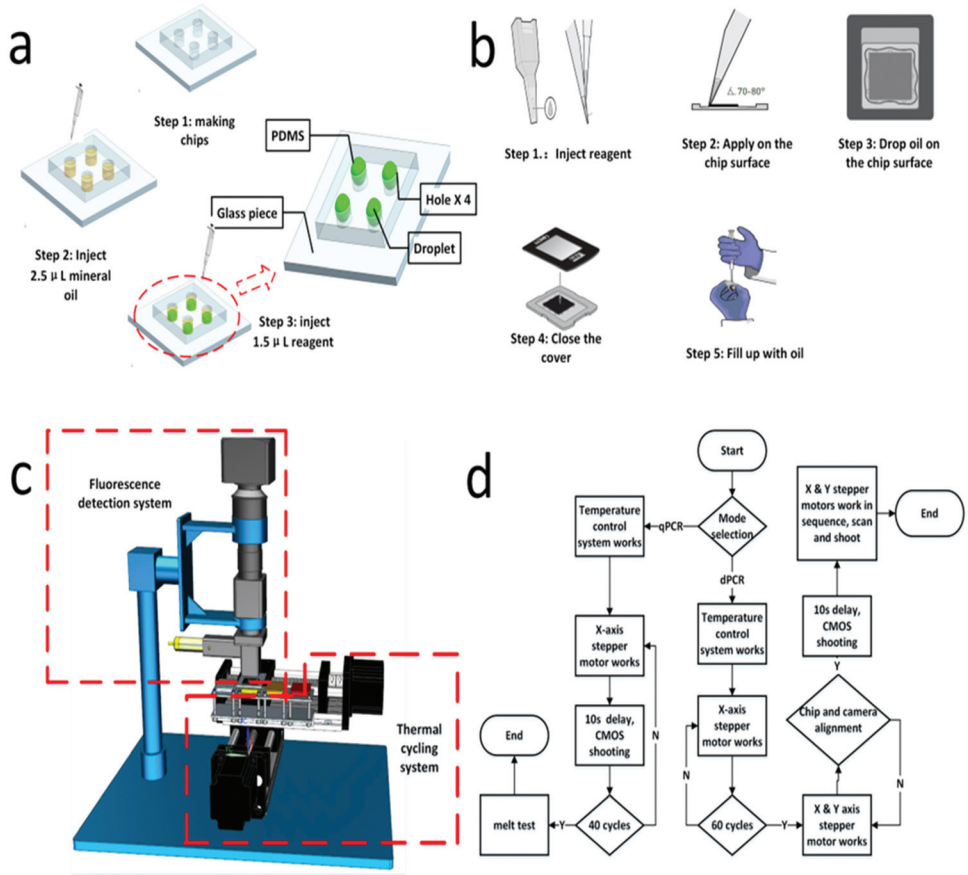

Fig. 1 Working mechanism and flow chart of self-made compound PCR detection equipment (a) the chip preparation for the qPCR mode. The chip used in the qPCR mode is made of PDMS and bonded to glass *via* a simple production method. (b) The commercial ABI chip preparation for the dPCR mode. (c) The overall structure of the compound PCR instrument. The fluorescence detection system (upper part) is responsible for the acquisition of the information whereas the thermal cycling system (lower part) is responsible for the gene amplification. (d) Control flow chart of the compound PCR instrument. The control system has an independent control flow depending on the mode selected.

Table 1 Part combination cost and specification model of self-made equipment

Part name	Specification and place of production	Price of self-made equipment ($)
CMOS camera	20 million pixel, Beijing, China	254
X–*Y* mechanical slider	EB1605, 100 × 100 mm, Beijing, China	87
Temperature controllers	TCMM207, Sichuan Province, China	231
Heating plates	PTC constant temperature heating plate, China	3
USB fan	CJY, China	2
Camera lens	50×–400× Zoom, Shenzhen, China	145
Laser	T850AD1670GD-P488, Shenzhen, China	60
Homogenizing tablet	T800-YHP-CFXPM015, Shenzhen, China	120
Filter	Narrow band filter, Beijing, China	55
Total price		957

apply the reagent to the chip surface and a layer of oil is added to the chip surface. Then, the lid is covered and the chip is filled with oil.

Two dimensional mechanical sliding table for temperature cycling and sequential actuation of the chip

The compound PCR instrument consists of two parts: a fluorescence detection unit and a temperature cycling unit (Fig. 1c). Since the fluorescence needs to be measured in each cycle of the qPCR mode whereas the dPCR mode only requires a fluorescence measurement at the end of the reaction, we divided the control system into two parts (Fig. 1d), for each mode (qPCR and dPCR).

Temperature cycling system. The temperature cycling system is mainly composed of two parts: the sliding thermal coupling mechanical structure and the constant temperature heat

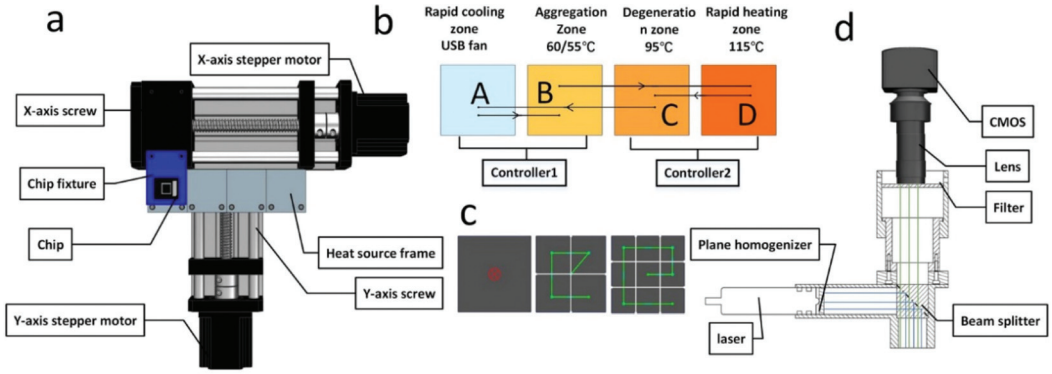

Fig. 2 Flow chart of digital PCR chip detection and image acquisition (a) mechanism of the sliding thermal mechanical coupling that determines the temperature cycling through reciprocating motions of the *x*-axis sliding table. (b) Constant temperature heat source. The constant temperature heat source is divided into four areas A: fast cooling area with an accelerating air flow using a USB fan. B: polymerization area where the single-stranded DNA combines with the primer and extends to form a double strand. C: denaturing area where the DNA opened into a single strand. D: fast heating area with the high-temperature heater. The black line represents the movement of the chip stage driven by the *x*-axis slide in a B–D–C–A–B pattern. (c) Scanning photograph of the *x*-axis and *y*-axis linkages in the dPCR mode. The black substrate is the chip, the green line represents the relative motion of the chip, and the white line represents the virtual boundary. (d) Fluorescence detection system. The system with a 20-megapixel CMOS camera to provide a sufficient resolution, a lens with a 4.5-time magnification, and a coaxial light source to provide a uniform illumination. Principle of the coaxial light source mechanism. The blue line is the laser beam and the green line represents the excited fluorescence. The laser irradiates the chip evenly and the emitted fluorescence is coaxial with the lens.

source. The thermal coupling structure consists of an *X*–*Y* mechanical slider (EB1605, 100 × 100 mm, Beijing, China), the chip holder (with a copper plate at the bottom), and the heat source holder (Fig. 2a). The constant temperature heat source includes three heating plates (PTC constant temperature heating plate, China), a USB fan (CJY, China), and two temperature controllers (TCMM207, Sichuan Province, China), as shown in Fig. 2b. Each heating chip is coated with thermal grease (HTWT160, Shenzhen, China) to improve the heat transfer between the heater chip and the chip stage. The requirements for temperature cycling are slightly different in each mode, but the implementation of temperature cycling is the same. Fig. 2b shows the motion path of the *x* axis slide. When the compound PCR instrument is in the qPCR mode, the USB fan is turned on and the temperature of the adjustable high temperature block is set to 115 °C. In the initial stages of the reaction, the chip is rapidly heated to 115 °C inside a rapid heating zone in 28 s. After the rapid heating, the chips are moved by the *x* axis slide table to a denaturation heating zone at 95 °C and stay there for 10 s. After the denaturation, the chip quickly moves back to the rapid cooling area with the USB fan for rapid cooling and stays there for 20 s. After cooling, the chip is moved to the polymerization area at 60 °C and maintained there for 35 s. This completes one temperature cycle (Fig. 2b). A cycle takes 93 s and a complete qPCR requires 40 cycles, which corresponds to 62 minutes. When the compound PCR instrument is in the dPCR mode, the temperature rise and fall rates must not exceed 2 °C s^{-1}. We set the temperature in the rapid region to 115 °C. In the initial stages of the reaction, the chip was pre-heated in the polymerization region at 55 °C for 120 s. After preheating, the chip enters the rapid heating zone at 115 °C and stays there for 90 s. After the rapid heating, the chip goes to the denaturation zone at 95 °C and stays there for 30 s. After denaturation, the chip quickly moves to the rapid cooling zone and stays there for 75 s. After the rapid cooling, it enters the polymerization zone at 55 °C and stays there for 67 s. It takes 167 s to complete a temperature cycle. It takes 60 cycles to complete a dPCR, which corresponds to 2.8 hours.

Sequential action of the chip. Scanning is a common method to obtain high-resolution images. The scanning action requires a relative motion of the chip and the camera. In this work, we used the *X*-axis and *Y*-axis links of a two-dimensional mechanical slider to move the chip and complete the scanning action. We divided the chip into 2 × 2 and 3 × 3 virtual regions (Fig. 2c). The initial position of the camera is in the middle of the chip. The *X*-axis and *Y*-axis sliders drive the chip to complete the scan. In the dPCR mode, the compound PCR instrument uses a Quantstudio 3D Digital PCR chip (Fig. 1b). The digital PCR chip has 20 000 microcavities with a total size of 10 × 10 mm. The operation of this chip is relatively simple and can be realized manually. The reagent addition process is as follows. First, a droplet of the reagent is added onto a dedicated loader, then the loader is used to apply the reagent to the chip surface and a layer of oil is added to the chip surface. Then, the lid is covered and the chip is filled with oil.

Fluorescence detection system

Although the compound PCR instrument must meet the requirements for the fluorescence detection of both modes, it will be suitable for the qPCR mode if it satisfies the requirements of the dPCR mode. The dPCR mode demands a higher level of performance from the fluorescence detection because the light source must evenly irradiate the chip and the camera must have a high resolution and a large magnification. However, the field-of-view of the camera is too small to capture

the whole chip. The fluorescence detection system designed in this work is composed of a laser light source, a coaxial light source structure, a CMOS (Complementary Metal–Oxide–Semiconductor) camera (E3ISPM, China), and a lens (Lapsun, Shenzhen, China), as depicted in Fig. 2d.

Uniform light. To achieve the uniform illumination of each droplet on the chip, we designed and manufactured a coaxial light source driven by the size of the lens in existing CMOS cameras. The coaxial light source includes a laser (T850AC1670GD-P488, Anford, China), a plane homogenizer (Anford, China), a filter (Hengyang optics, China), a spectroscope (Hengyang Optics), and a lens (Fig. 2d). The planar homogenizer expands the circular laser source into square spots. The center wavelength of the laser is 480 nm. The laser is reflected by the spectroscope while the 480 nm light is totally reflected so that the laser evenly irradiates the chip. The laser excited fluorescence with a wavelength of about 500 nm passes through the spectroscope and the filter to reach the lens of the CMOS lens and is then captured by the CMOS sensor.

Scanning photography to overcome the small field-of-view. The dPCR chip of the compound PCR instrument has 20 000 microreaction chambers and the droplet volume in the chip is at pL levels. Therefore, a high resolution CMOS camera and a large-magnification lens must be used for the fluorescence detection. This means the field-of-view of the camera will be small, which makes it impossible to record only one image at a time. We used scanning photography to solve this problem. As the chip moves in sequence, the CMOS camera takes pictures in turn. Finally, by processing the images recorded, a complete photograph can be reconstituted to lift the contradiction between a high resolution and a large field-of-view.

Melting curve analysis in the qPCR mode

The dye used in the qPCR mode is not specific and will bind to any double-stranded DNA. The melting curve determines whether or not there is non-specific amplification. After the qPCR reaction, we adjust the temperature of the heating piece from 60 °C to 95 °C in steps of 1 °C lasting 5 s each. The fluorescence intensity is measured once. The temperature change is realized by a program and the fluorescence intensity is analyzed by the computer.

Results and discussion

Bubbles during the use of the qPCR chip

Bubbles are the first problem that must be solved in PDMS chips.[23] In the related study,[24,25] researchers modified the chip surface to make the chip surface hydrophobic. Mineral oil droplets were formed on the hydrophobic chip surface to form spherical oil droplets with a large contact angle. The sample is then injected into oil droplets to form a closed reaction chamber. However, this method is too complicated and requires a long hydrophobic treatment on the chip surface, which is costly. Here, we had eliminated bubbles well. During qPCR, the reagents produced a large number of bubbles in the reaction wells (Fig. 3). At the high temperature of the denaturation stage, the bubbles rapidly expand and burst, causing the reagent to squeeze out of the reaction hole and the test to fail. We believe that when PDMS is bonded to the glass plate, the lower surface of the PDMS (edge of the hole) is damaged during the opening of the hole, which results in the presence of gas at the edge of the reaction hole. When the temperature rises, the gas expands and enters the reagent. We solved this problem by changing the order of the addition of the reagents. We first added the mineral oil and then added reagents. This solves the formation of air bubbles in the wells of the qPCR reaction and improves the experimental success rate.

Comparison of the compound PCR instrument and commercial qPCR system

In this work, nucleic acids were amplified by a two-step method. Fig. 4a shows the actual temperature cycle curve of

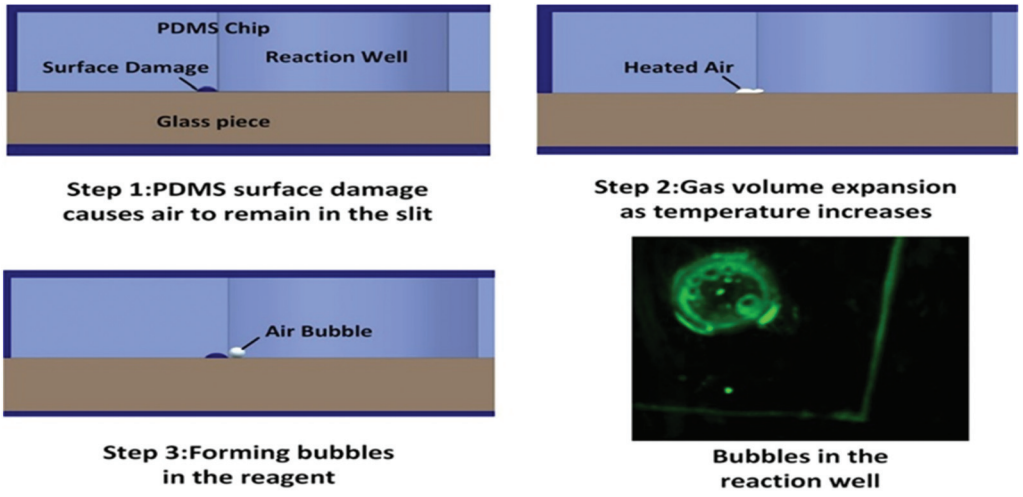

Fig. 3 Cross-sectional view of bubble formation process in reaction wells.

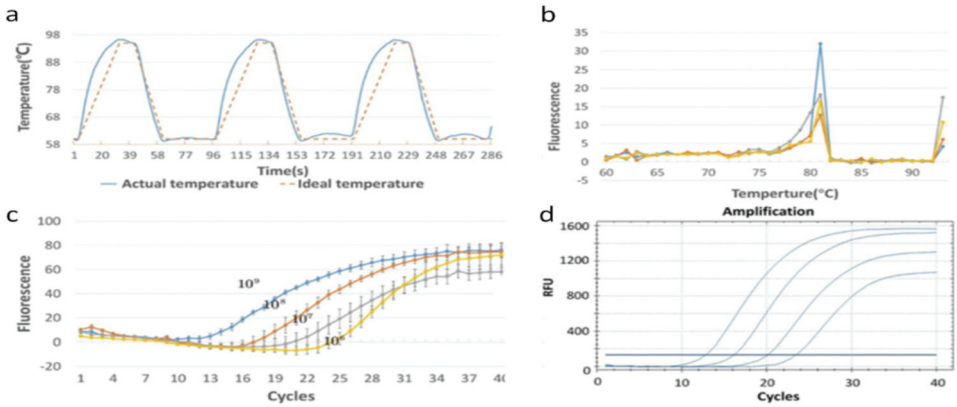

Fig. 4 Result analysis diagram of real-time fluorescence detection of compound PCR equipment (a) temperature cycling curve for the compound PCR instrument in the dPCR mode. (b) The melting curve with peaks appearing around 81 °C indicating a specific amplification. (c) Gradient concentration experiment in the qPCR mode with a relatively uniform interval for the cycles for the different concentrations. (d) Gradient concentration experiment on the commercial qPCR system.

the compound PCR instrument. The two key temperatures of 95 °C and 60 °C are well maintained and there is no temperature overshoot. We amplified the same reagent on the compound PCR instrument and a commercial real-time fluorescent PCR instrument with the same temperature cycle and the same number of cycles (40). We selected three groups to determine the shown in Fig. 4b. There are no significant differences with the commercial qPCR instrument (Fig. 4c). We defined the fluorescence threshold at 20 for the compound PCR unit to provide the threshold cycle Ct. The values of Ct for the compound PCR are 15.7, 20.1, 24.2, and 27.3 whereas the Ct for the commercial qPCR was 12.8, 16.13, 20.09, and 23.40. Although the Ct values of the two instruments are different in value, the differences between the Ct values of the different curves of the two instruments are similar. To test the reaction products of the compound PCR instrument, we recorded melting curves (Fig. 4d). The melting curves show very close peaks, at about 81 °C, in the intensity attenuation at different concentrations, which indicates specific products.

The reaction effect of compound PCR instrument in dPCR mode

During the dPCR test, we used two commercial dPCR instruments (QuantStudio 3D digital PCR system, ABI; DropX-1000, Rainsure) to perform amplification tests on UPE-Q reagents. Experimental results are not ideal, and the two instruments do not draw the scatter diagrams of fluorescence intensity. When analyzing the reason for the failure of the test, we performed the same experiment using the compound PCR instrument. The advantage of this is that we can get the original image, and the original image can help us to find the reason why the commercial instrument can't get the reaction result. Through our own instruments, we found that the threshold line of this reagent was difficult to determine. Because the threshold cannot be determined, the experimental results cannot be obtained, which shows that UPE-Q reagents are not suitable for dPCR experiments on these two commercial instruments.

Actual temperature cycling effect. Fig. 5a shows the actual temperature cycling curve of the compound PCR instrument in the dPCR mode. The two key temperatures, namely 95 °C and 55 °C, are stable. The rise and fall rates are fast enough for dPCR with an appropriate temperature plateau. We performed an amplification on the compound PCR instrument using the Quantstudio 3D Digital PCR chip and took a fluorescence image of the chip. The results of the thermal profile of the digital PCR chip (Fig. 6) are shown as follows:

Scanning photography improves the accuracy of droplet recognition. We used two methods to image the chip: a fixed shooting (1 × 1) and a zone scanning photography (2 × 2 and 3 × 3). We stitched the images obtained by scanning photography and zoomed in the same position in all three images (Fig. 5b). The edges of the image obtained by the fixed shooting are blurred and the light is uneven, whereas the quality of the images obtained by scanning photography is much higher. We selected a region of interest in each of the three photos on the same edge. And then we used ImageJ (a software, ImageJ is a public image processing software based on java, which is developed by the National Institutes of Health) to identify the droplets on the chip. A large number of droplets are lost in the images obtained by the fixed shooting, but almost all the droplets are recognized in the image obtained by scanning. This shows that scanning photography can effectively improve the accuracy of droplet recognition, which lays a foundation for the subsequent fluorescence intensity statistics of each droplet.

Eliminating the influence of uneven illumination by regional fluorescence intensity analysis. We used scanning photography to solve the problem of inaccurate point recognition. Although we used coaxial light sources to improve the problem of uneven illumination, there is still a problem of strong light in the middle of the field of view and weak light at the edges (Fig. 5c). This problem seriously affects the determination of the fluorescence threshold and leads to the failure of

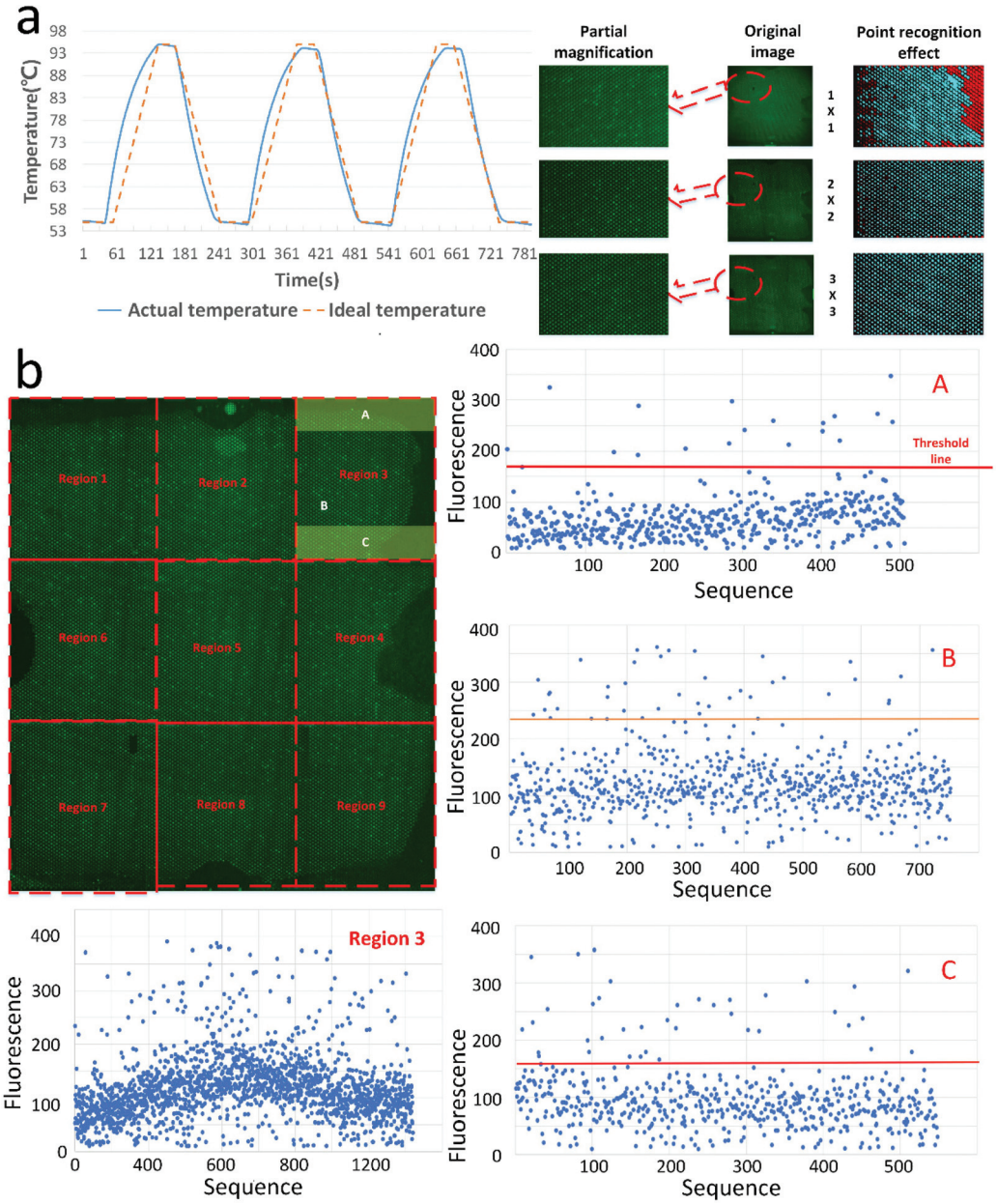

Fig. 5 Flow chart of image acquisition and analysis mechanism for digital PCR detection of compound PCR equipment (a) actual temperature cycle in the dPCR mode. The temperature in the denaturation zone is 95 °C. The temperature in the polymerization zone is 55 °C. (b) Advantage of scanning photography. When the same area of 1 × 1, 2 × 2, and 3 × 3 images are enlarged, the quality of the 3 × 3 image is highest. With the scanned image, the identification of the droplets is more accurate (red represents unrecognized, and blue represents recognized). (c) The effect of regional statistics. The scatter diagram of fluorescence intensity in region 3 shows the phenomenon of middle high and edge low, which indicates that the illumination is very uneven. The scatter plots of area *A*, *B*, and *C* are close to straight lines, indicating that the illumination is uniform.

commercial dPCR detection. To solve this problem, we did not directly analyze the stitched images but divided each scanned image into three regions: A, B, and C. The A and C regions are the edge regions of the image. Analyzing these three areas, we could see that the lighting is very uniform. This lays the foundation for the determination of the fluorescence threshold.

Determine threshold by reverse reasoning. At present, commercial digital PCR instruments use complex algorithms to determine the fluorescence threshold and use this threshold to identify each droplet on the whole chip. However, the uneven illumination on the chip cannot be completely avoided. The brightness of the positive drop on the edge may not reach the threshold value. The system mistakenly determines the positive drop as the negative drop, which results in a statistical error.

We used the method of reverse reasoning to get a real and reliable threshold. The process of reverse reasoning was shown in Fig. 7a. Each point in the scatter chart has a certain relation-

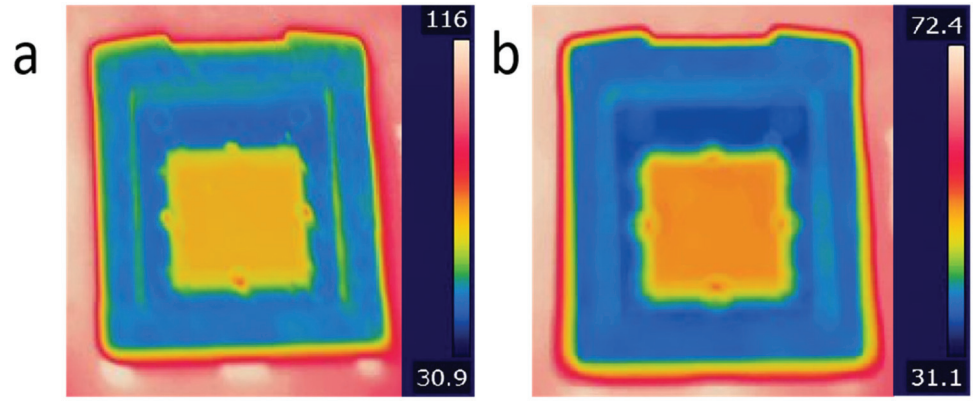

Fig. 6 Thermal homogeneity diagram of digital PCR chip. Figure a shows the heat distribution when the chip is in the denatured region during the PCR cycle. Figure b shows the thermal distribution of the chip when it is in the annealing region during the PCR cycle.

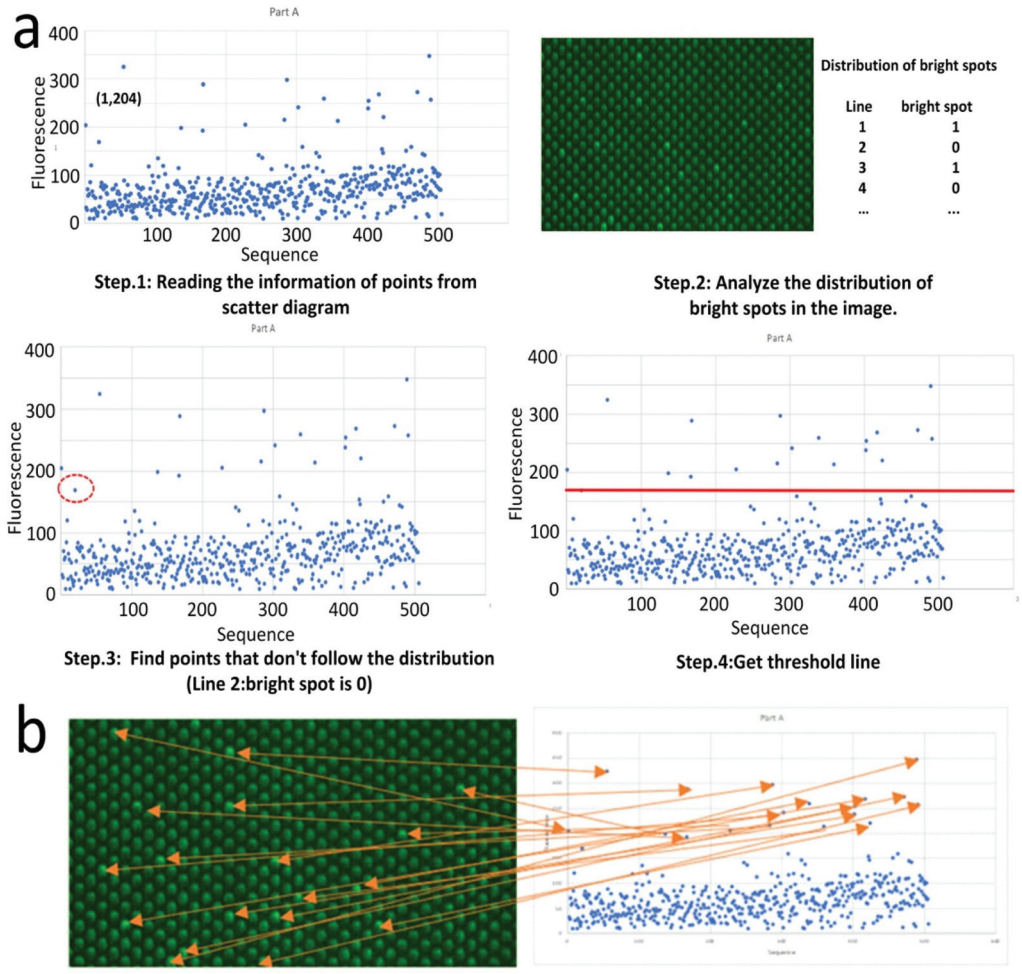

Fig. 7 Result analysis diagram of digital PCR detection of compound PCR equipment (a) the steps of threshold determination. (b) Bright spot recognition effect. The bright points obtained according to the threshold, which can be seen to be consistent with the real bright points.

ship with each point in the image. The abscissa of each point in the scatter chart is arranged from left to right for each line in the image, and 19 is the number of points in a line in the image. Dividing the abscissa of the scattered point by 19 could easily get the position in the image. The method of statistical fluorescence intensity in different regions and the method of threshold determination based on converse reasoning can effectively eliminate the influence of uneven illumination. For part A of region 3, we

determined the threshold to be 169, and the points with fluorescence intensity greater than 169 in the scatter plot were bright points, and these bright points could correspond to the original image one-to-one (Fig. 7b). By adding the number of bright spots and dark spots in different regions, we can get the number of bright spots and dark spots in the whole chip. The number of positive droplets we obtained was 1096, and the total number of droplets was 18 319. After calculation, we obtained the initial concentration of the sample as 1208 copies per μL. The concentration of the reagent we added is 1000 copies per μL, which shows that the results obtained by the compound PCR instrument in dPCR mode are reliable.

Conclusions

In this paper, it is proved that it is feasible to set up a compound PCR instrument that integrates the functions of qPCR and dPCR. The stable temperature cycle and high-resolution fluorescence detection were realized by using a two-dimensional mechanical slide. This kind of compound PCR instrument has good performance in qPCR mode, but there is still room for improvement in dPCR mode.

We used the mechanical slide not only to realize the temperature cycle but also to improve the problem of uneven illumination. Compared with fixed photography, when the number of scanning photography is increased, the image quality is greatly improved, however, in the dPCR mode, there are still some shortcomings in the scanning photography of 3 × 3 for the reagents with a fuzzy threshold. We solved this problem perfectly by the method of regional statistics and the reverse reasoning threshold. And we have realized the detection of reagents that cannot be detected by commercial dPCR. Besides, we think that further subdividing the area and using scanning to obtain more partial images (4 × 4, 5 × 5,...) may help solve this problem. In the next work, we will verify this idea and try to get higher quality images.

For the absolute quantification of genes whose threshold is not obvious, experiments have confirmed that by using our fluorescence analysis method, the accuracy of droplet identification can be effectively improved.

In general, the compound PCR instrument realized the integration of qPCR and dPCR, which can not only achieve high sensitivity nucleic acid detection (dPCR mode), but also has a large detection range (qPCR mode). At the same time, the low price of hardware and software makes it easier to promote. In this paper, we proposed an idea to realize the integration of qPCR and dPCR based on a two-dimensional slide, and the corresponding control and analysis methods. Based on this idea, we will further optimize this new method and system to achieve more sample analysis.

Conflicts of interest

No conflict of interest exits in the submission of this manuscript, and manuscript is approved by all authors for publication.

Acknowledgements

This project is supported by the talent program from Guangdong Academy of Sciences (2021GDASYL-20210102012) and GDAS' Project of Science and Technology Development (2022GDASZH-2022010110).

References

1 K. Kleppe, E. Ohtsuka, R. Kleppe, I. Molineux and H. G. Khorana, Studies on polynucleotides: XCVI. Repair replication of short synthetic DNA's as catalyzed by DNA polymerases, *J. Mol. Biol.*, 1971, **56**(2), 341–361, DOI: 10.1016/0022-2836(71)90469-4.

2 R. K. Saiki, *et al.*, Enzymatic amplification of beta-globin genomic sequences and restriction site analysis for diagnosis of sickle cell anemia, *Science*, 1985, **230**(4732), 1350–1354, DOI: 10.1126/science.2999980.

3 C. Qian, *et al.*, A fast and visual method for duplex shrimp pathogens detection with high specificity using rapid PCR and molecular beacon, *Anal. Chim. Acta*, 2018, **1040**, 105–111, DOI: 10.1016/j.aca.2018.07.064.

4 H. Larsen, N. B. Goecke and C. K. Hjulsager, in *Subtyping of Swine Influenza Using a High-Throughput Real-Time PCR Platform and a Single Microfluidics Device, in Nucleic Acid Detection and Structural Investigations: Methods and Protocols*, ed. K. Astakhova and S. A. Bukhari, Springer US, New York, NY, 2020, pp. 17–25.

5 K. E. Dingle, X. Didelot, T. P. Quan, *et al.*, A role for tetracycline selection in recent evolution of agriculture-associated Clostridium difficile PCR ribotype 078[J], *mBio*, 2019, **10**(2), e02790-18.

6 X. Li and Y. Guan, Specific Identification of the Adulterated Components in Beef or Mutton Meats Using Multiplex PCR, *J. AOAC Int.*, 2019, **102**(4), 1181–1185, DOI: 10.5740/jaoacint.18-0338.

7 I. Hein, G. Flekna, M. Krassnig and M. Wagner, Real-time PCR for the detection of Salmonella sin food: An alternative approach to a conventional PCR system suggested by the FOOD-PCR project, *J. Microbiol. Methods*, 2006, **66**(3), 538–547, DOI: 10.1016/j.mimet.2006.02.008.

8 P. M. Fratamico, *et al.*, Evaluation of a Multiplex Real-Time PCR Method for Detecting Shiga Toxin–Producing Escherichia coli in Beef and Comparison to the U.S. Department of Agriculture Food Safety and Inspection Service Microbiology Laboratory Guidebook Method, *J. Food Prot.*, 2014, **77**(2), 180–188, DOI: 10.4315/0362-028X.JFP-13-248.

9 K. Masago, *et al.*, Validation of the digital PCR system in tyrosine kinase inhibitor-resistant EGFR mutant non-small-cell lung cancer, *Pathol. Int.*, 2018, **68**(3), 167–173, DOI: 10.1111/pin.12630.

10 W. Liu, *et al.*, A multiplex PCR method mediated by universal primers for the identification of eight meat ingredients in food products, *Eur. Food Res. Technol.*, 2019, **245**(11), 2385–2392, DOI: 10.1007/s00217-019-03350-9.

11 C.-S. Liao, G.-B. Lee, H.-S. Liu, T.-M. Hsieh and C.-H. Luo, Miniature RT–PCR system for diagnosis of RNA-based viruses, *Nucleic Acids Res.*, 2005, **33**(18), e156–e156, DOI: **10.1093/nar/gni157**.

12 P.-L. Quan, M. Sauzade and E. Brouzes, dPCR: A Technology Review, *Sensors*, 2018, **18**(4), 4, DOI: **10.3390/s18041271**.

13 T. Xu, *et al.*, A PDMS-based digital PCR chip with vacuum aspiration and water-filling cavity integrated for sample loading and evaporation reduction, in *2018 IEEE Micro Electro Mechanical Systems (MEMS)*, 2018, pp. 1142–1145, DOI: **10.1109/MEMSYS.2018.8346763**.

14 J. Hu, *et al.*, Proximity ligation assays for precise quantification of femtomolar proteins in single cells using self-priming microfluidic dPCR chip, *Anal. Chim. Acta*, 2019, **1076**, 118–124, DOI: **10.1016/j.aca.2019.05.034**.

15 H. Li, *et al.*, Versatile digital polymerase chain reaction chip design, fabrication, and image processing, *Sens. Actuators, B*, 2019, **283**, 677–684, DOI: **10.1016/j.snb.2018.12.072**.

16 M. Cereda, *et al.*, Q3: A Compact Device for Quick, High Precision qPCR, *Sensors*, 2018, **18**(8), 8, DOI: **10.3390/s18082583**.

17 R. A. Mendoza-Gallegos, A. Rios and J. L. Garcia-Cordero, An Affordable and Portable Thermocycler for Real-Time PCR Made of 3D-Printed Parts and Off-the-Shelf Electronics, *Anal. Chem.*, 2018, **90**(9), 5563–5568, DOI: **10.1021/acs.analchem.7b04843**.

18 A. Salman, H. Carney, S. Bateson and Z. Ali, Shunting microfluidic PCR device for rapid bacterial detection, *Talanta*, 2020, **207**, 120303, DOI: **10.1016/j.talanta.2019.120303**.

19 S. Zhou, *et al.*, A highly integrated real-time digital PCR device for accurate DNA quantitative analysis, *Biosens. Bioelectron.*, 2019, **128**, 151–158, DOI: **10.1016/j.bios.2018.12.055**.

20 S. H. Lee, *et al.*, Bubble-free rapid microfluidic PCR, *Biosens. Bioelectron.*, 2019, **126**, 725–733, DOI: **10.1016/j.bios.2018.10.005**.

21 S.-Y. Ma, *et al.*, Peanut detection using droplet microfluidic polymerase chain reaction device, *J. Sens.*, 2019, DOI: **10.1155/2019/4712084**.

22 K. Wang, D. Wu and W. Wu, A New Self-Activated Micropumping Mechanism Capable of Continuous-Flow and Real-Time PCR Amplification Inside 3D Spiral Microreactor, *Micromachines*, 2019, **10**(10), 10, DOI: **10.3390/mi10100685**.

23 W. Wu, K.-T. Kang and N. Y. Lee, Bubble-free on-chip continuous-flow polymerase chain reaction: concept and application, *Analyst*, 2011, **136**(11), 2287–2293, DOI: **10.1039/C0AN01034K**.

24 L. He, B. Sang and W. Wu, Battery-Powered Portable Rotary Real-Time Fluorescent qPCR with Low Energy Consumption, Low Cost, and High Throughput, *Biosensors*, 2020, **10.5**, 49, DOI: **10.3390/bios10050049**.

25 J. An, *et al.*, Low-Cost Battery-Powered and User-Friendly Real-Time Quantitative PCR System for the Detection of Multigene, *Micromachines*, 2020, **11.4**, 435, DOI: **10.3390/mi11040435**.